JOURNAL OF AGRICULTURAL AND FOOD CHEMISTRY

J. Agric. Food Chem. **2004,** *52,* 823−831 **823**

Wheat Flour Enzymatic Amylolysis Monitored by in Situ ^{1}H NMR Spectroscopy

MARIA E. AMATO,[†] GIULIANA ANSANELLI,[‡] SALVATORE FISICHELLA,[†] RAFFAELE LAMANNA,*[,‡] GIUSEPPE SCARLATA,[†] ANATOLI P. SOBOLEV,[§] AND ANNALAURA SEGRE[§]

Dipartimento di Scienze Chimiche, Università Viale A. Doria, 6-95125 Catania, Italy, CR ENEA Trisaia UTS Biotec-Agro, SS 106 Jonica Km 419.5, 75026 Rotondella (Mt), Italy, and Institute of Chemical Methodologies, CNR, M.B. 10, 00016 Monterotondo Stazione, Rome, Italy

Starch enzymatic degradation caused by endogenous hydrolases is studied by in situ NMR spectroscopy on a set of hard and soft wheat flours. The results obtained by two different techniques (HR-MAS and ^{1}H NMR in solution) are analyzed in terms of a Michaelis−Menten kinetic phenomenological model taking into account the presence of endogenous enzymes and their eventual inactivation. The parameters resulting from the best fit of all experimental data to the kinetic model equations are submitted to a multivariate statistical analysis to assess the role of the oligosaccharides release in distinguishing between hard and soft wheats.

KEYWORDS: Wheat flour; hydrolyzing enzymes; ^{1}H NMR; HR-MAS; statistical analysis

INTRODUCTION

Wheat is one of the most extensively used cereals for the preparation of bread and bakery products worldwide. In particular, hard wheats are preferred for boiled foodstuffs and soft wheats for baked products. Starch constitutes the major component of wheat seeds, where it provides the energy for germination. To make use of the chemical energy stored in starch, organisms need starch hydrolyzing enzymes (hydrolases). The hydrolytic activity of enzymes on native starch granules affects all levels of food processing and nutritional qualities. Rheological properties of dough, loaf volume, staling of breadcrumb, and the rate of firming during storage are only a few of the technological aspects influenced by enzymes.

With the intention of improving the methods for the quality assessment of wheat, the amylolytic starch degradation, due to endogenous hydrolases, on hard and soft wheat flours is studied.

In this paper, the kinetic release of oligosaccharides is monitored in hydrated flours by in situ NMR spectroscopy. This technique has the advantage of providing, in a single spectrum, qualitative and quantitative information on mixtures of several compounds already present or formed during the enzymatic reaction (*1*). Two different experimental methods are used: HR-MAS and ^{1}H NMR in solution. In the latter method, only the amount of oligosaccharides diffused in the buffer solution is measured, while in the HR-MAS spectra, all molecules with a sufficient mobility are observed, even if they are still embedded in the polysaccharidic matrix. For HR-MAS, the sample preparation does not require any chemical procedure or extraction, therefore possible side-effects arising from drying or non continuous extractive procedures are avoided, while in the solution experiment, a simple on-line water extraction is accomplished. To study the enzymatic hydrolysis of carbohydrates in wheat flours, we monitor the amount of few mono and oligosaccharides as a function of the time. In fact, the concentration of these saccharides is much larger than that of the enzymes which, due to their low concentration, cannot be directly observed. Finally, the results obtained by the two techniques are analyzed in terms of a kinetic model and submitted to a statistical treatment.

MATERIALS AND METHODS

Samples. Wheat flour samples are gifts from Istituto di Cerealicoltura (Rome, Italy) and University of Viterbo (Italy). After elimination of impurities and broken grains, each wheat sample is conditioned with tap water overnight to 16.5% of final humidity and milled by means of a laboratory scale mill (Bühler MLU-202, Uznil Switzerland).

Two different sets of samples are prepared, depending on the NMR technique used.

For HR-MAS, 100 μL of 100 mM phosphate buffer solution in D_2O (pH 6.8) are mixed with 50 mg of flour to obtain a homogeneous sample. This sample is packed into a 4 mm HR-MAS rotor, with 12 μL spherical insert, and analyzed about 30 min after preparation.

For high-resolution liquid-state NMR, flour sample (50 mg) is suspended in 1 mL of phosphate buffer solution in D_2O, pH 6.8, and swirled gently for 1 min. This suspension is transferred

* To whom correspondence should be addressed. Fax +39 0835 974724. E-mail: raffaele.lamanna@trisaia.enea.it.
[†] Università Viale A. Doria
[‡] CR ENEA Trisaia UTS Biotec-Agro.
[§] Institute of Chemical Methodologies.

10.1021/jf035188v CCC: $27.50
Published on Web 01/23/2004

into an NMR tube and used after 30 min from the preparation when two well separated phases are observed due to flour sedimentation.

The same temperature, pH and concentration conditions are used within each group of experiments, performed by ^{1}H NMR in solution and HR-MAS in soft matter.

NMR Techniques. HR-MAS NMR spectra are recorded on a Bruker 600 Avance spectrometer operating at 600.13 MHz at 300 K. The proton HR-MAS spectra are collected with a 90° pulse of 5 μs, a relaxation delay of 2 s, 64 scans, and a spinning rate of 5 kHz. To suppress the strong residual HOD signal, the presaturation is applied during the relaxation delay. To monitor the enzymatic hydrolysis of starch, a set of 42 ^{1}H NMR spectra is acquired for each sample, allowing a 5 min delay between consecutive experiments. The delay between the beginning of the enzymatic reaction and the registration of the first proton HR-MAS spectrum is 30 min.

Two-dimendional NMR (2D NMR) experiments (COSY, TOCSY, and HSQC) are performed as previously reported (*11*).

^{1}H NMR solution spectra on flour suspensions are recorded at 300 K with a Varian UNITY Inova-500 instrument operating at 499.88 MHz. DSS is used as internal reference.

During the relaxation delay, to suppress the HOD residual signal, a presaturation sequence is applied. To monitor the enzymatic hydrolysis of starch, a set of 15 ^{1}H NMR spectra is acquired for each sample, allowing a 45 min delay between consecutive experiments. The delay between the beginning of the enzymatic reaction and the registration of the first proton spectrum is 30 min. 2D NMR experiments (COSY, TOCSY, and HSQC) are performed using standard procedures in the phase sensitive mode. The processing is performed using the Varian VNMR software (version 6.1 C).

DOSY experiments are performed in solution at 600 MHz by a bipolar LED sequence with sine shaped gradient pulses of different intensities. The gradient amplitude (g) is changed from 1.6 to 28.9 G cm^{-1} in 32 constant steps. The time-of-flight and the gradient pulse duration are $\Delta = 100$ ms and $\delta/2 = 2$ ms, respectively. The delay between the two bipolar gradient pulses is $\tau = 400$ μs. Sixteen transients are co-added with a recycle delay of 2 s. The FIDs are apodized using an exponential line broadening of 5 Hz and Fourier transformed by a Zoom FFT algorithm. The spectrum of each experiment is fitted, by a least-squares minimization algorithm, with a sum of Lorentzian lines, and the corresponding intensities are plotted against the gradient strength. The diffusion coefficient of each spectral line is calculated by fitting the intensity versus gradient curve by the following equation:

$$A = \sum_j A_{oj} \exp\left(-D_j q^2 \left(\Delta - \frac{\delta}{3} - \frac{\tau}{2}\right)\right) \quad \text{where } q = \gamma g \delta$$

The DOSY spectrum is reconstructed by using Gaussian line shapes in the *D* dimension centered at the diffusion coefficient and having a half-height line-width equal to half of the error on *D*. In the frequency dimension, the least-squares fit of the experiment with the lowest gradient strength is used.

HR-MAS spectra can be easily calibrated because the intensity of the resonances corresponding to fatty acids does not change as a function of time and can be used for internal calibration.

In solution NMR spectra quantitative measurements are performed by direct integration with respect to an unassigned singlet at 0.15 ppm whose intensity does not change as a function of time.

Best Fit of Kinetic Data. The best fit of the kinetic experimental data is accomplished by a simultaneous non linear regression of β-maltose and β-glucose concentrations, using eqs 1 and 2 (see Kinetic Interpretation). The χ^2 of β-maltose is calculated with eq 1 and that of β-glucose with eq 2. The best fit parameters are extracted by minimizing the sum of both χ^2 values, by varying the set of five parameters. The minimization algorithm used is the "Nelder−Mead simplex method", implemented on Matlab software (The MathWorks Inc.). The simultaneous fit of both, β-maltose and β-glucose data, by the same model, reduces the correlation between the five parameters, and as a consequence, the possibility of data overfitting.

Confidence limits on estimated model parameters are calculated by a Monte Carlo simulation of synthetic data sets. For each real data set, starting from the corresponding best fit parameters, 100 synthetic data sets are created by using eqs 1 and 2 and by adding random numbers, with a variability comparable with the standard deviation between the original and the best fit data. For each synthetic data set, the best fit parameters are extracted and the confidence limits are calculated as a standard deviation of the results on the entire Monte Carlo data set.

Statistical Methods. Data of HR-MAS and ^{1}H NMR in solution are submitted to statistical analysis by using Statistica software package for Windows (1997 edition by Statsoft, Inc.), to determine if and in what extent the kinetic variables are able to distinguish between hard and soft wheats. Multivariate Analysis of Variance (MANOVA), Tree Clustering Analysis (TCA) and Linear Discriminant Analysis (LDA) are used to treat the data.

MANOVA is applied to the data set with the aim of selecting variables with a significant discriminant power. The *F* and *p*-level parameters are used to perform the selection. In particular, the *F* value is defined as the ratio of the "between-groups variability" and "within-group variability". The larger is the ratio, the larger is the discriminant power of the corresponding variable. The *p*-level gives the probability of error involved in accepting the result; a low *p*-level corresponds to a high probability that the relationship between samples is reliable.

TCA, applied to the selected variables, classifies samples without any a priori hypothesis, to check how they naturally group according to an amalgamation rule. In this work, the "complete linkage" method is used to determine when two clusters are sufficiently similar to be joined together.

LDA allows the determination if the model is capable of distinguishing between a priori defined groups (i.e., if the formed clusters are significantly different). Moreover, by LDA, it is possible to establish which variables have significantly different means across the groups.

The discriminating power is given by the Wilks' Lambda factor, whose value ranges from 0.0, which corresponds to a perfect discriminating power, to 1.0, which indicates no discriminating power for the model.

This technique, applied to the selected kinetic variables, is used to rank all samples among the two a priori defined groups of soft and hard wheats.

RESULTS AND DISCUSSION

HR-MAS ^{1}H NMR at 600 MHz. In the HR-MAS conditions, at 600 MHz, hydrated wheat flour (soft matter) shows a proton spectrum that can be analyzed in terms of lipids and of carbohydrates (**Figure 1**).

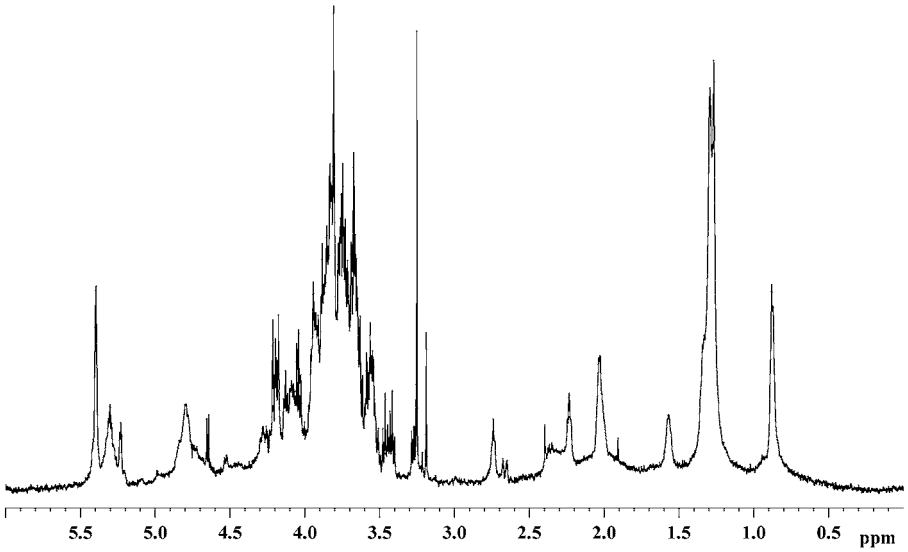

Figure 1. HR-MAS spectrum of a wheat flour sample in phosphate buffer, spun at 5 kHz.

Table 1. Proton Chemical Shift Assignments of Water/Wheat Flour Mixtures[a]

molecule	assignment	^{1}H shift HR-MAS	^{13}C shift HR-MAS	^{1}H shift soln	^{13}C shift soln
lipids	terminal CH_3	0.87			
lipids	backbone methylene groups	1.25			
lipids	(–CH_2–CH_2–CO–O-)	1.55			
lipids	(–CH_2–CH═CH-)	2.00			
lipids	(–CH_2–CH_2–CO–O-)	2.20			
lipids	(–CH═CH–CH_2–CH═CH-)	2.72			
β-glucose	C2	3.26	75.2	3.26	75.1
β-glucose	C4	3.40	70.7	3.38	70.7
α-glucose	C4	3.41	70.7	3.42	70.7
β-glucose	C1	4.64	96.9	4.64	97.0
β-maltose	C1, reducing end	4.65		4.66	97.1
α-glucose	C1	5.23	93.1	5.24	93.0
α-maltose	C1, reducing end	5.23	93.1	5.23	93.1
lipids	(–CH_2–CH═CH-)	5.32			
α-maltose	C1, non reducing end	5.41	101.0	5.41	100.8
β-maltose	C1, non reducing end	5.41	101.0	5.41	100.8
carbohydrates	non reducing ends	5.35–5.50			

[a] Only selected resonances are reported.

The assignment of the carbohydrates is performed using literature data (*2*, *3*) and confirmed by 2D COSY, TOCSY, and ^{1}H-^{13}C HSQC maps. The spectral assignments are reported in **Table 1**.

In contrast with previously reported data (*4*), the system (wheat flour and phosphate buffer) is not stable but shows some resonances clearly increasing with time.

As shown in **Figure 2**, the resonances due to the lipid fraction have constant intensities, while those due to the sugar moieties increase as a function of time. The kinetic behavior of the system can be explored by measuring, in the spectra, the intensities of the β-glucose and β-maltose anomeric protons reducing-end as function of time. In fact, these signals are well resolved, while all the other carbohydrate signals show big overlaps; actually, also the α-glucose and the α-maltose anomeric reducing ends appear as an isolated doublet.

In all samples, the β-maltose and β-glucose signals show an initially fast increasing intensity, which progressively increases more slowly until a plateau is reached. In **Figure 3**, the intensities of the β-glucose and β-maltose anomeric peaks are reported as functions of time for several wheat samples.

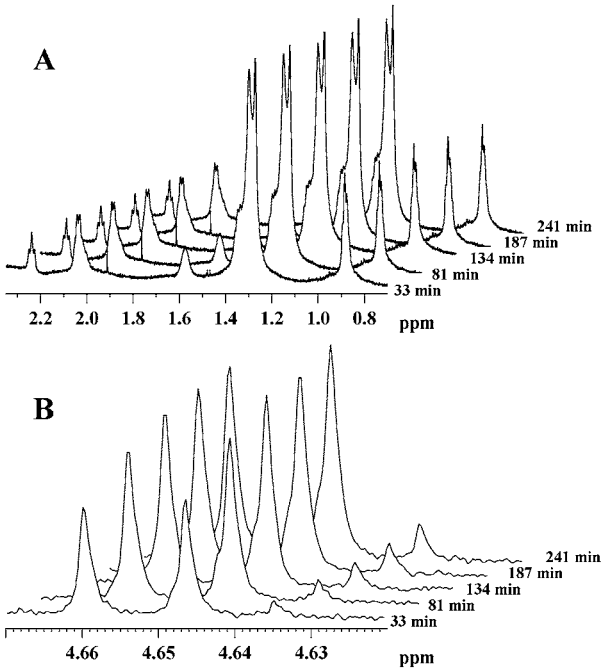

Figure 2. Stack plot of ^{1}H HR-MAS spectra of a wheat flour sample at different times of the enzymatic kinetic: (A) expansion of the region corresponding to the lipids, (B) expansion of the region corresponding to the β-glucose and β-maltose anomeric signals.

^{1}H NMR in solution at 500 MHz. Figure 4 shows the ^{1}H NMR spectrum of a two-phase sample of flour in phosphate buffer: the solid hydrated flour is on the bottom of the NMR tube, outside the NMR coil, while the solution is in the active section of the probe.

In this spectrum, all lines previously attributed to fatty chains are not present. The only observable resonances are those due to the dissolved glucose, maltose, and short-chain polysaccharides. The assignment, reported in **Table 1**, agrees with literature data (*2*, *3*) and is confirmed by 2D COSY, TOCSY, and ^{1}H-^{13}C HSQC experiments.

As in the case of HR-MAS spectra, we observe an increment of the carbohydrates concentration as a function of time.

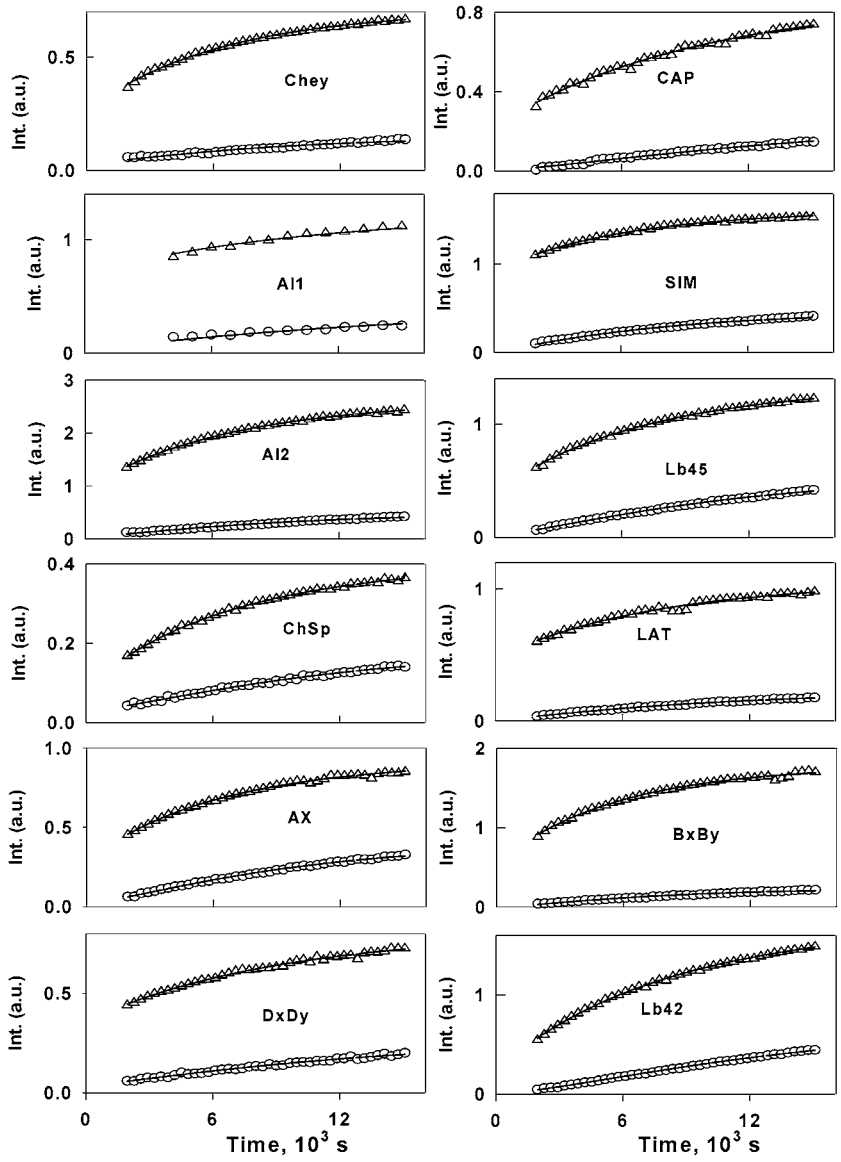

Figure 3. Intensities of the β-glucose (open circles) and β-maltose (open triangles) anomeric signals, as a function of time, for several wheat samples. The solid lines represent the best fit of data to eqs 1 and 2.

In **Figure 5**, the intensity of β-glucose and β-maltose anomeric protons signals is reported as a function of time for several samples; a plateau is reached only after several hours.

In solution spectra, the absence of a significant contribution of β-reducing units of low molecular weight maltodextrins to the anomeric signal of maltose is confirmed by DOSY experiments (**Figure 6**). Such a contribution cannot be excluded in the case of HR-MAS. Actually, due to restricted diffusion, no well-resolved DOSY maps are obtainable in soft matter; in fact, restricted diffusion provides apparent diffusion coefficients, whose values are determined by the size and the shape of the barrier rather than by the shape of the diffusing molecules (*5*, *6*).

In addition, the non reducing end signals of carbohydrates in HR-MAS spectra show a more complex pattern with respect to the corresponding solution signals. This suggests that polysaccharides of longer chains became visible in HR-MAS spectra (see **Figure 7**) due to the suppression of chemical shift anisotropy by magic angle spinning.

Kinetic Interpretation. To describe the kinetic behavior of oligosaccharides in hydrate flour, we need two phenomenological equations that connect maltose and glucose concentration to time.

The enzymatic pathways that lead to maltose and glucose are very complex and involve many carbohydrates species, several endogenous enzymes, and some inhibitors (*7*−*9*). The mathematical description of such a system requires a very complex system of nonlinear differential equations whose solution cannot be obtained analytically (*7*). However, it is possible to describe the experimental data by considering a simple phenomenological model, as described in the Appendix, in which an average behavior is considered (i.e., the system is described as if only two enzymes were present and working on a single substrate). This is indeed a large approximation, but it permits a good phenomenological set of analytical equations that fit the experimental data and provide suitable numerical parameters to be used in the statistical analysis to be obtained.

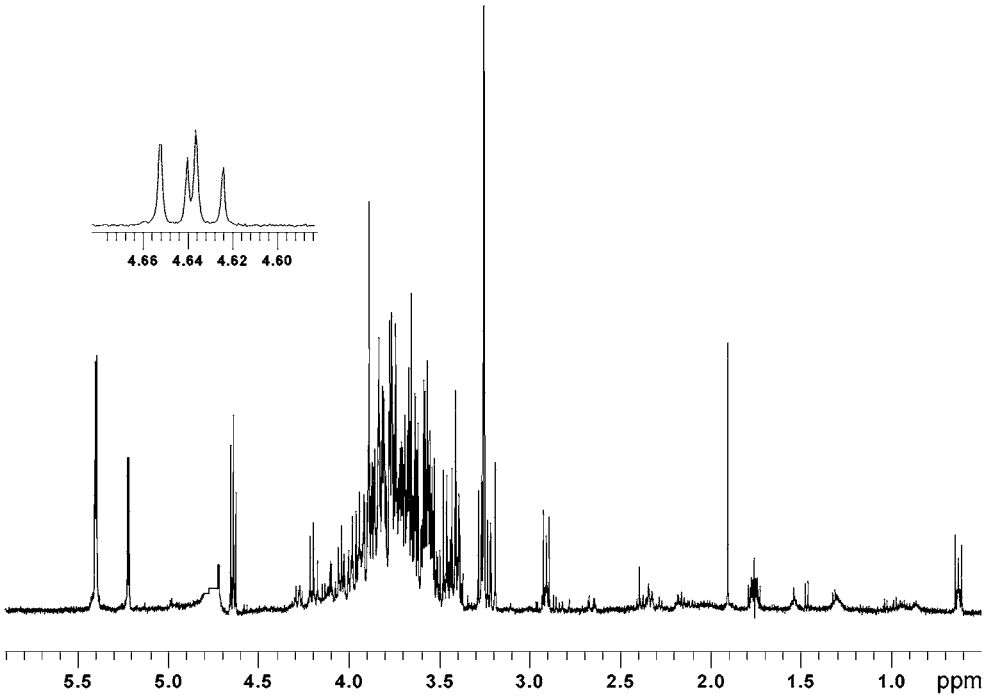

Figure 4. ^{1}H NMR spectrum of the liquid portion (phosphate buffer) in a two-phase wheat flour sample.

We assume that the reactions that transform starch into maltose and maltose into glucose obey the Michaelis−Menten equation and that the enzymes involved in the reactions are progressively inactivated, according to a 1st-order chemical process (*10*).

From the solution of the two linearized kinetic differential equations for our model (see Appendix), we obtain the following relationships, which give the concentration of maltose and glucose as a function of the time:

$$M(t) = \frac{V_{M_0}K_M}{V_{G_0}} - \left(\frac{V_{M_0}K_M}{V_{G_0}} - M_0\right)e^{-(V_{G0}/\alpha K_M)(1-e^{-\alpha t})} \quad (1)$$

$$G(t) = G_0 + \frac{V_{M_0}}{\alpha}(1 - e^{-\alpha t}) - \left(\frac{V_{M_0}K_M}{V_{G_0}} - M_0\right)(1 - e^{-(V_{G0}/\alpha K_M)(1-e^{-\alpha t})}) \quad (2)$$

Six unknown parameters appear in eqs 1 and 2: M_0 and G_0 are the concentrations of maltose and glucose before the starting of the enzymatic reactions, respectively; V_{M_0} and V_{G_0} are the maximum velocity for maltose and glucose formation in the absence of inactivation, respectively; K_M is the Michaelis−Menten constant for the maltases; and α is the inactivation 1st-order constant for both amylases and maltases. A best fit of the experimental data is obtained by using five independent parameters, namely, V_{M_0}, V_{G_0}/K_M, α, M_0, and G_0, because V_{G_0} and K_M appear always as a ratio in both equations.

The parameters resulting from a best fit of all experimental data to eqs 1 and 2 are reported in **Table 2** and **Table 3** for HR-MAS and solution experiments, respectively.

For the sake of clarity, we will discuss the two sets of data, soft matter and solution, separately, and the obtained results will be compared only at the end of the discussion.

Statistical Interpretation. The kinetic parameters extracted from the best fit of NMR data are submitted to a multivariate statistical analysis to assess the role of the oligosaccharides release in distinguishing between hard and soft wheats.

In particular, the MANOVA analysis of the five kinetic parameters (M_0, G_0, V_{M_0}, α, and V_{G_0}/K_M) obtained from HR-MAS spectra, shows that G_0 is the only discriminant variable with respect to wheat hardness. The G_0 variable is associated with a high F value of 45.8 and a very low p-level of 4.9×10^{-5}.

In **Figure 8** the G_0 parameter is plotted for each wheat sample.

The plot clearly shows that soft wheats have a G_0 value much larger than those of the hard wheats. In particular, for the soft wheat group, the G_0 average is 2.4, with a standard deviation of 0.6, while the G_0 average for the hard wheats is 0.2, with a standard deviation of 0.3.

The MANOVA analysis of solution state data indicates M_0, V_{M_0} and G_0 as the most significantly discriminant parameters for wheat hardness.

A TCA is carried out in this case by using the M_0, V_{M_0} and G_0 parameters suggested by MANOVA. In **Figure 9**, we report the dendrogram obtained from TCA. If the tree is cut at a first level, it shows Alisei 1 well separated from all other flours. By cutting the dendrogram at a lower level, two clusters are obtained, exhibiting a good separation between soft and hard wheats, with the exception of the cultivar (cv) Chinese Spring, a soft wheat falling in the hard wheat group. The Euclidean distance is used to form clusters.

Since Alisei 1 does not belong to any group, we exclude this sample from LDA, to avoid its influence in determining the discriminant power of the model between hard and soft wheats.

The LDA, applied to the selected variables, shows a clear separation among soft and hard wheats (see **Figure 10**), even if the two groups are rather near to each other and the confidence limit curves indicate some overlap. The Wilks' Lambda value (0.4) suggests a fair discriminant power for the model and the F value (6.4) is greater than F critic, implying that the groups means differ more than would be expected by chance alone.

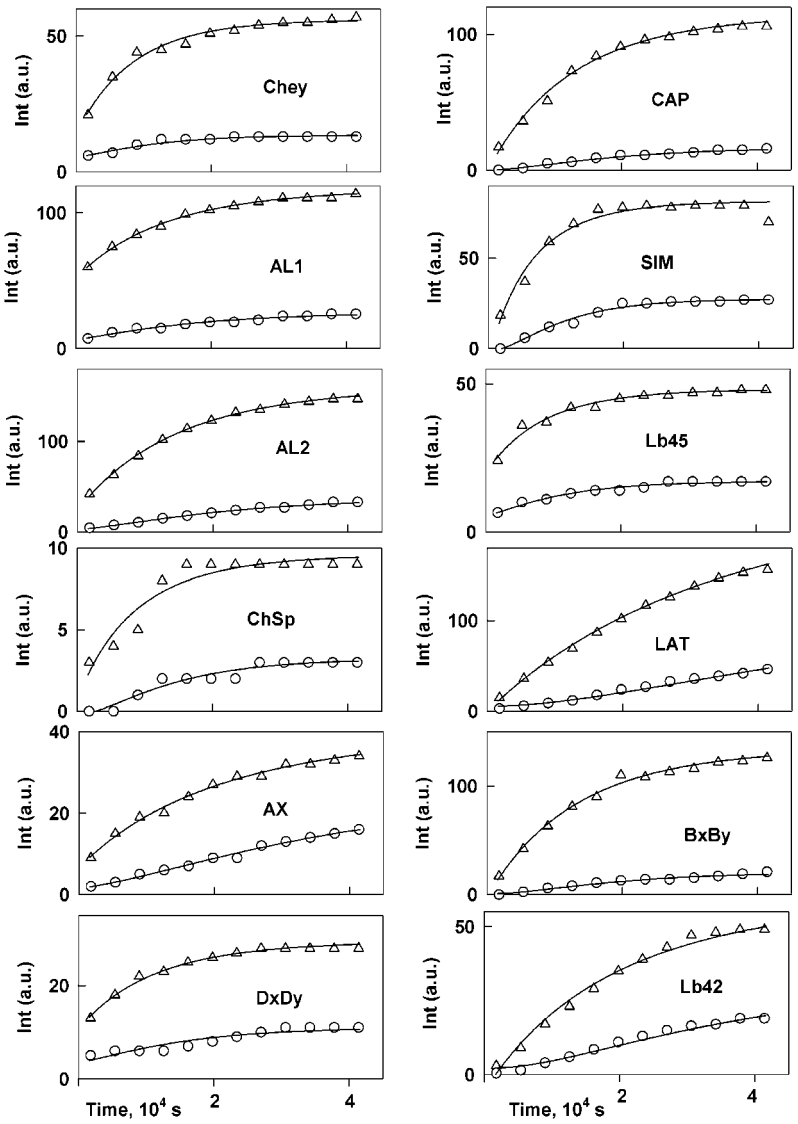

Figure 5. Intensities trend, as function of time, of the β-glucose (open circles) and β-maltose (open triangles) anomeric signals, in the solution conditions, for all the wheat samples considered. The solid lines represent the best fit of data to eqs 1 and 2.

Table 2. Kinetic Parameters of Enzymatic Hydrolysis of Wheat Flour Starch in Soft Matter Conditions

flour	group[a]	V_{M_0} $\times 10^5$	σ $\times 10^5$	V_{G_0}/K_M $\times 10^5$	σ $\times 10^5$	α $\times 10^5$	σ $\times 10^5$	M_0 $\times 10^2$	σ $\times 10^2$	G_0 $\times 10^2$	σ $\times 10^2$
DxDy	S	6.4	0.6	3.6	0.4	9.0	1.0	35	1	3.1	0.5
AX	S	12.9	0.6	7.6	0.4	12.0	1.0	28	1	1.2	0.5
ChSp	S	5.4	0.3	6.6	0.4	11.3	0.6	9	1	2.8	0.2
Chey	S	8.2	0.5	3.5	0.3	14.3	0.8	26	1	2.8	0.4
AL1	S	7.4	1.0	3.0	0.4	8.2	0.8	69	4	2.6	1.9
AL2	S	29	1.0	3.4	0.2	13.3	0.6	94	3	2.0	1.0
SIM	H	17	2.0	5.1	0.5	14.0	1.0	91	2	0.0	1.4
BxBy	H	24	2.0	3.3	0.3	16.0	1.0	55	5	0.0	6
CAP	H	7.8	0.9	3.6	0.4	8.0	2.0	22	2	0.0	0.4
LAT	H	9.6	0.9	3.3	0.4	12.0	2.0	47	2	0.6	0.4
Lb42	H	20.7	0.7	6.0	0.2	9.2	0.4	24	2	0.0	
Lb45	H	16.8	0.8	6.5	0.3	11.1	0.7	39	2	0.8	0.6

[a] S, soft wheat; H, hard wheat.

The reliability of this result is good, as indicated by the *p*-level value that is smaller than 0.02.

Comparison of Experimental Data Sets. In the two experimental methods, HR-MAS and solution NMR, the observed kinetic curve shape (see **Figures 3** and **5**), and consequently, the five fitting parameters (see **Tables 2** and **3**) are different. These differences can be rationalized in terms of the different reaction conditions in the two sets of experiments and in the diffusion process that brings soluble molecules to the liquid phase. In fact, the reaction conditions are quite different in soft matter and in the two phase samples. In soft matter, all the reaction products and inhibitors remain confined in the solid matrix and in intimate contact with the enzyme molecules. On the other hand, in the two phase experiments,

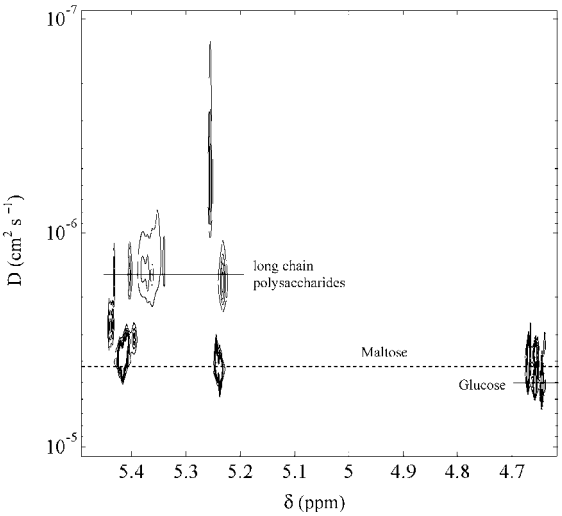

Figure 6. DOSY spectrum of the wheat flour sample in solution condition: expansion of the region corresponding to the anomeric resonances.

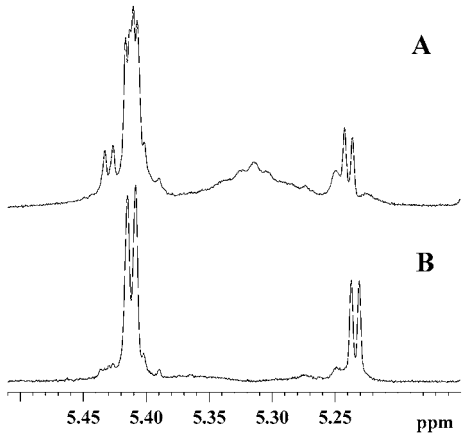

Figure 7. A comparison between HR-MAS spectrum (A) and ^{1}H NMR solution spectrum (B) of a wheat flour sample. The HR-MAS spectrum shows a more complex pattern with respect to the corresponding solution signals. In particular, in the HR-MAS spectrum, are clearly visible the signals due to the lipids double bond protons (–CH═CH-) at 5.32 ppm and some signals at 5.41 ppm, overlapping the anomeric peaks of maltose and glucose, probably due to polysaccharides of longer chains.

Table 3. Kinetic Parameters of Enzymatic Hydrolysis of Wheat Flour Starch in Aqueous Suspension

flour	group[a]	V_{M_0} $\times 10^3$	σ $\times 10^3$	V_{G_0}/K_M $\times 10^5$	σ $\times 10^5$	α $\times 10^5$	σ $\times 10^5$	M_0	σ	G_0	σ
DxDy	S	2.1	0.2	3.0	0.4	7.8	0.7	10.6	0.7	3.3	0.6
AX	S	1.9	0.1	2.9	0.2	3.4	0.4	6.6	0.7	1.5	0.3
ChSp	S	1.3	0.3	3.5	0.8	3.6	0.9	0.0	2.8	1.4	0.5
CHEY	S	5.6	0.6	2.5	0.4	11.0	1.0	14.0	2.0	5.4	0.4
AL1	S	5.9	0.3	1.6	0.1	7.0	0.4	52	1.0	6.4	0.6
AL2	S	10.1	0.4	2.2	0.1	5.9	0.3	24.0	2.0	2.7	0.4
SIM	H	14.0	2.0	8.0	1.0	12.0	1.0	–6.0	5.0	–0.8	0.9
BxBy	H	10.3	0.8	2.1	0.2	6.6	0.5	0.0	4.0	0.0	0.6
CAP	H	9.6	0.8	2.1	0.2	7.3	0.6	–2.0	4.0	0.2	0.4
LAT	H	7.2	0.3	1.8	0.1	2.0	0.2	0.0	2.0	5.5	0.8
Lb42	H	3.4	0.3	3.2	0.4	3.6	0.5	–6.0	2.0	2.4	0.6
Lb45	H	3.5	0.2	4.8	0.3	8.8	0.3	–0.7	0.6	0.9	0.3

[a] S, soft wheat, H, hard wheat.

both products and inhibitors are diluted in the liquid phase. Therefore, the inhibition process should be attenuated in the two phase experiments by dilution with an increment of the

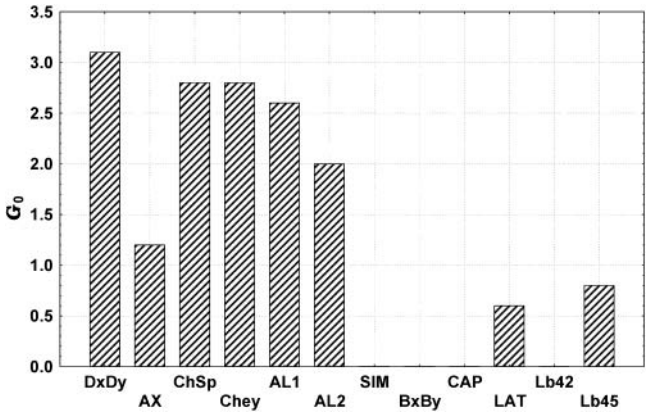

Figure 8. Bar plot representing the G_0 values as a function of the wheat sample; soft wheat are reported on the left side.

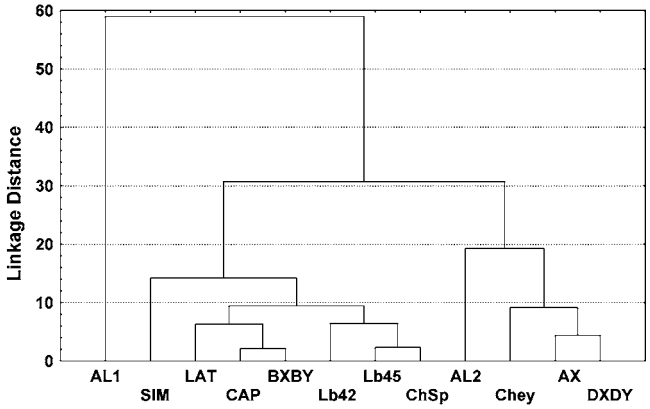

Figure 9. Dendrogram from TCA analysis of the wheat flour samples kinetic parameters.

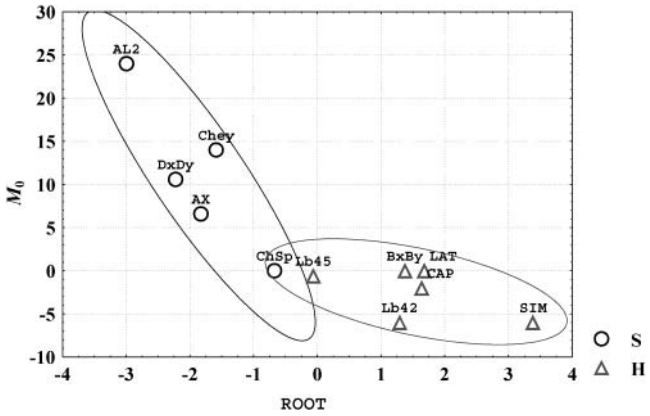

Figure 10. LDA scatter plot of the wheat flour samples obtained using the M_0, V_{M_0} and G_0 variables suggested by MANOVA. Ellipses represent 95% confidence regions for each group.

time in which the concentration plateau is reached. This is in agreement with the fact that the α parameter, which is inversely proportional to the time in which the plateau is reached, is systematically higher in soft matter with respect to solution experiments.

Moreover, due to the diffusion process, which brings the glucose and maltose into the liquid phase, the sugar concentration observed in the solution might not be comparable with that observed in soft matter. For these reasons, it is impossible to directly compare the fitting results obtained in soft matter and in solution. In fact, except for α, whose difference has been already discussed, the other parameters are concentration

dependent and their absolute value depends on the experimental conditions. However, despite the fact that fitting parameters obtained in the two sets of experiments have different absolute value, they contain similar information on the enzymatic degradation of wet flour. Actually, from the statistical analysis of the two kinds of experiments, similar results are obtained on the role of botanic origin of the wheat on the enzymatic degradation of starch. In particular, both NMR methods show a clear discrimination between hard and soft wheat.

CONCLUSIONS

The enzymatic degradation of polysaccharides in hydrated wheat flours is monitored by in situ NMR spectroscopy. By considering a phenomenological model for the kinetic behavior of glucose and maltose, some kinetic parameters are extracted and analyzed by multivariate statistical methods to exploit the contribution of botanical origin of wheat to the starch degradation in hydrated flours. Two NMR methods are used to monitor the change of glucose and maltose concentration during the enzymatic activity, and both methods show a good sensitivity to the vegetal origin of the flour.

Statistical analyses show that the only discriminant variable for the HR-MAS system is G_0, while for the solution data set, V_{M_0}, M_0 and G_0 result to be the most discriminant variables. These results indicate that the initial concentrations, M_0 and G_0, are the principal variables capable of distinguishing between soft and hard wheats. Moreover, in the solution case, also V_{M_0}, the maximum velocity for maltose formation in the absence of enzymes inactivation, contributes to the discrimination. On the contrary, α, the inactivation 1st-order constant for the enzymes, is never involved in the discriminant model, suggesting that the enzyme inactivation is not conditioned by the wheat vegetal origin.

Depending on the botanical origin, starch granules show different susceptibilities to amylase hydrolysis and different kinetics of degradation, suggesting a relationship of such behaviors with the molecular properties of starch and with the hardness of wheats.

The study of the time evolution of the NMR signals in the hydrated flour wheat, together with the application of a suitable phenomenological model allows the evaluation of initial metabolite concentrations even in time unstable food samples. Actually, the initial concentrations of glucose and maltose, which are sensible to the botanical origin of wheat, could be determined by NMR by only applying the above-described method.

At our knowledge, this is the first attempt to use kinetic parameters, measured with NMR methods, to separate a class of foodstuff according to its features of processing and conversion.

We plan to check the above observations enlarging our data set and trying to optimize the experimental procedures.

ABBREVIATIONS USED

cv, cultivar; AL1, Alisei 1 Bx7-Dy12-Dx2; AL2, Alisei2 Bx7-Dy12; Chey, Cheyenne Dx5-Ax2*-Bx7-By9-Dy10; ChSp, Chinese Spring Dx2 −Bx7 −By8 − Dy1; DxDy, WRU 6979 DX5-DY10; AX, WRU 6981 AX1; CAP, Capeiti; LAT, Latino; SIM, Simeto; SIM, Simeto; BxBy, Lira BX20-BY20; Lb42, Lira b 42; Lb45, Lira b 45

APPENDIX

The Kinetic Model. In the NMR spectra of wheat flour, we observe a monotonic change of maltose and glucose concentration as a function of time. This variation is attributed to an enzymatic activity triggered by the flour sample hydration. We assume that the evolution of the system is determined by two coupled enzyme reactions represented by the following system of nonlinear differential eqs (*12*):

$$\frac{dM}{dt} = f(S,M,t) - g(M,t)$$

$$\frac{dG}{dt} = g(M,t) \qquad \text{(A1)}$$

where $f(S,M,t)$ represents the transformation of starch or long chain polysaccharide (S) into β-maltose (M) and $g(M,t)$ represents the transformation of maltose into glucose (G). The explicit time dependence takes into account enzyme inhibition or inactivation.

The shape of the f and g functions depends on the kind of reaction involved in the transformation.

If the enzyme works according to the Michaelis−Menten model, without inhibition or inactivation, the shape of f and g function is the following:

$$f(S,M) = V_M \frac{S}{S + K_S}$$

$$g(M) = V_G \frac{M}{M + K_M} \qquad \text{(A2)}$$

where V_M and V_G are the maximum velocity for maltose and glucose formation, respectively, and K_S and K_M are the Michaelis−Menten constants for the reactions which transform long chain polysaccharides into maltose and maltose into glucose, respectively.

Because in the wheat flour, the starch content is very high with respect to low molecular weight carbohydrates, the following condition is satisfied:

$$S \gg K_S \qquad \text{(A3)}$$

On the other hand, the maltose is produced enzymatically from starch; thus, its concentration, at least at the beginning of the reaction, is very low, and the following condition should be satisfied:

$$M \ll K_M \qquad \text{(A4)}$$

If conditions A3 and A4 are satisfied during the reactions, eq A2 can be written as:

$$f(S,M) = V_M$$

$$g(M) = V_G \frac{M}{K_M} \qquad \text{(A5)}$$

The maximum velocity of the reaction is related to the concentration of active enzyme that complexes the substrate.

$$V = k_{cat} E_a \qquad \text{(A6)}$$

where E_a is the active enzyme concentration.

In the case of enzyme inhibition or inactivation, the maximum velocity could become time dependent. In particular, if a 1st-order kinetic model is considered for the enzyme inactivation, the concentration of active enzyme results from the following

eq (*10*):

$$E_a \xrightarrow{k_i} E_i$$

$$\frac{dE_a}{dt} = -k_i E_a \qquad \text{(A7)}$$

$$E_a = E_0 e^{-k_i t}$$

Taking into account eqs A6 and A7 and the conditions A3 and A4, in the case of 1st-order inactivation kinetics, the functions f and g become

$$f(S,M,t) = V_{M_0} e^{-k_{iM} t}$$

$$g(M,t) = V_{G_0} e^{-k_{iG} t} \frac{M}{K_M} \qquad \text{(A8)}$$

where V_{M_0} and V_{G_0} are the maximum velocity for maltose and glucose formation in the absence of inactivation, respectively.

From the NMR data as a function of time, it results that both maltose and glucose reach the concentration plateau at approximately the same time, indicating that $k_{iM} \sim k_{iG}$.

By combining eqs A1 and A8 and assuming $k_{iM} = k_{iG} = \alpha$, we have the following equations:

$$\frac{dM}{dt} = V_{M_0} e^{-\alpha t} - V_{G_0} e^{-\alpha t} \frac{M}{K_M}$$

$$\frac{dG}{dt} = V_{G_0} e^{-\alpha t} \frac{M}{K_M} \qquad \text{(A9)}$$

These are linear equations whose solutions are

$$M(t) = \frac{V_{M_0} K_M}{V_{G_0}} - \left(\frac{V_{M_0} K_M}{V_{G_0}} - M_0 \right) e^{-(V_{G0}/\alpha K_M)(1-e^{-\alpha t})} \qquad \text{(A10a)}$$

$$G(t) = G_0 + \frac{V_{M_0}}{\alpha}(1 - e^{-\alpha t}) - \left(\frac{V_{M_0} K_M}{V_{G_0}} - M_0 \right)(1 - e^{-(V_{G0}/\alpha K_M)(1-e^{-\alpha t})}) \qquad \text{(A10b)}$$

where M_0 and G_0 are the concentrations of maltose and glucose before the starting of the enzymatic reactions, respectively.

Some consideration on the validity of eq A4 can be obtained by calculating the function $g(M,t)$ of eq A1 from the experimental data as the numerical derivative of glucose concentration. In all our kinetic data, we found that $g(M,t)$ is a monotonically decreasing function; this shows that the formation rate of glucose is dominated by the inactivation contribution. In fact, according to eqs A2 and A5, the reaction velocity is expected to be a monotonically increasing function of M. In the early stage of the reaction, the approximation in eq A4, which is necessary only to make analytically tractable the differential equation system in eq A1, reasonably holds, while at longer time the inactivation mechanism makes the velocity of reaction so close to zero that the use of eq A2 or A5 is inessential.

The main point for the interpretation of our kinetic data is the appearance of a plateau in the concentration versus time plot, which means that the velocity of reaction goes to 0 after a certain amount of time. This behavior cannot be explained by a simple inhibition that brings the system to work at a non null constant reaction rate at long times.

LITERATURE CITED

(1) Spangenberg, P.; Chiffoleau-Giraud, V.; Andre, C.; Dion, M.; Rabiller, C.; Probing the transferase activity of glycosidases by means of in situ NMR spectroscopy. *Tetrahedron*: *Asymmetry* **1999**, *10*, 2905−2912.

(2) Sugiyama, H.; Nitta, T.; Horii, M.; Motohashi, K.; Sakai, J.; Usui, T.; Hisamichi, K.; Ishiyama, J. The conformation of α-(1−4)-linked glucose oligomers from maltose to maltoheptaose and short-chain amylose in solution. *Carbohydr. Res.* **2000**, *325*, 177−182.

(3) Fan, T. W.-M. Metabolite profiling by one- and two-dimensional NMR analysis of complex mixtures. *Prog. Nucl. Magn. Reson. Spectrosc.* **1996**, *28*, 161−219.

(4) Sacco, A.; Neri Bolsi, I.; Massini, R.; Spraul M.; Humpfer, E.; Ghelli, S. Preliminary Investigation on the characterization of Durum Wheat flours coming from some areas of south Italy by means of 1H−high-resolution magic angle spinning nuclear magnetic resonance. *J. Agric. Food Chem.* **1998**, *46*, 4242−4249.

(5) Callaghan, P. T. In *Principle of Nuclear Magnetic Resonance Microscopy*; Clarendon Press: Oxford, 1991.

(6) Johnson, C. S., Jr. Diffusion ordered nuclear magnetic resonance spectroscopy: principles and applications. *Prog. Nucl. Magn. Reson. Spectrosc.* **1999**, *34*, 203−256.

(7) Beltrame, P. L.; Calniti, P. Kinetic of enzymic hydrolysis of malto-oligo-saccharides: a comparison with acid hydrolysis. *Carbohydr. Res.* **1987**, *166*, 71−83.

(8) Yook, C.; Robyt, J. F. Reactions of alpha amylases with starch granules in aqueous suspension giving products in solution and in a minimum amount of water giving products inside the granule. *Carbohydr. Res.* **2002**, *337*, 1113−1117.

(9) Hill, G. A.; Macdonald, D. G.; Lang, X. α-amylase inhibition and inactivation in barley malt during cold starch hydrolysis. *Biotechnol. Lett.* November **1997**, *19*, 1139−1141.

(10) Schokker, E. P.; van Boekel, M. A. J. S. Kinetic modeling of enzyme inactivation: kinetics of heat inactivation at 90−110 °C of extracellular proteinase from Pseudomonas fluorescens 22F. *J. Agric. Food Chem.* **1997**, *45*, 4740−4747.

(11) Sobolev, A. P.; Segre, A.; Lamanna, R.; Proton high-field NMR study of tomato juice. *Magn. Reson. Chem.* **2003**, *41*, 237−245.

(12) Guide, G. M.; Goldbeter, A. From bistability to oscillations in a model for the isocitrate dehydrogenase reaction. *Biophys. Chem.* **1998**, *72*, 201−210.

Received for review October 14, 2003. Revised manuscript received December 5, 2003. Accepted December 8, 2003. Financial support provided by Italian MURST ex 60% (Progetto di Ricerca di Ateneo).

JF035188V